International Conference on Applied Energy 2021
Nov. 29 - Dec. 5, 2021, Thailand/Virtual
Paper ID: 014

3D-Printed Zeolite NaX-Magnesium Chloride Units as Ammonia Carriers

Zhejian Cao*, Rafael Acosta Laisequilla, Farid Akhtar*

Division of Materials Science, Luleå University of Technology, 97187 Luleå, Sweden

*Corresponding author: Z. Cao (zhejian.cao@ltu.se); F. Akhtar (farid.akhtar@ltu.se)

ABSTRACT

Ammonia (NH_3) has been reported as promising hydrogen storage media for clean fuel applications and is widely used as a reductant in selective catalytic reduction (SCR) systems. With such a huge potential in various environmental-friendly applications, however, ammonia is facing several challenges in its storage and delivery feasibility. In this study, we have designed three-dimensional (3D) printed zeolite NaX (faujasite)-magnesium chloride ($MgCl_2$) structured units by the pressure-assisted micro-syringe method. The 3D printed unit consists of a NaX scaffold and $MgCl_2$ blocks located inside, where the NaX scaffold provides the space to accommodate the volume swing during ammonia adsorption-desorption cycles, $MgCl_2$ to $Mg(NH_3)_6Cl_2$ to $MgCl_2$. The 3D printed unit demonstrates a net-zero structural change and offers structural stability during ammonia adsorption-desorption cycles. Moreover, by combining the zeolite and metal ammine complexes, we demonstrate that physisorption and chemisorption of ammonia occur in structured units and offer high sorption capacity and rapid kinetics in ammonia adsorption and desorption.

Keywords: ammonia, SCR, 3D printing, zeolite, hydrogen storage

1. INTRODUCTION

Air pollution has raised severe concern in recent years, especially after several air pollutants, such as nitrogen oxides (NO_x) and fine particulate matter ($PM_{2.5}$), have been reported correlated to the incidence and mortality of coronavirus disease 2019 (COVID-19) [1,2]. Therefore, efficient approaches to eliminate NO_x emissions and clean fuels are of desire. Ammonia (NH_3) is one of the most common reductants used for NO_x abatement in selective catalytic reduction (SCR) systems [3], and it has also been recognized as a high-density hydrogen storage material [4,5]. As one of the most produced base chemicals (approximately 144 million tons globally in 2020) [6], ammonia demonstrates great potential in both environmental and energy-related applications.

Ammonia is a hazardous gas with a pungent odor and requires safe and reliable high-capacity storage with a rapid-dosing storage media to expand its applied scenarios. Conventional SCR system uses urea ($(NH_2)_2CO$) solution as an indirect ammonia source, revealing various problems recently, such as low converting efficiency by the exhaust cooling, urea residues damaging the SCR catalyst, urea solution frozen at low temperature, and carbon dioxide (CO_2) emission [7–9]. Emerging ammonia carriers, alkaline earth metal halides (AEMHs), such as $MgCl_2$, $SrCl_2$, and $CaCl_2$, have been widely studied and industrialized as ammonia carriers for automotive SCR systems owing to the direct ammonia dosing and superior ammonia capacity [10–12]. Nevertheless, to meet the increasingly stringent NO_x emission standard, AEMHs require enhancement in their structural stability and the dosing kinetics [13]. During the ammonia absorption-desorption cycles, the AEMHs have dramatic volume swing, e.g., around 400 % volume expansion from $MgCl_2$ (41 $cm^3\ mol^{-1}$) to $Mg(NH_3)_6Cl_2$ (157 $cm^3\ mol^{-1}$) [14]. With this devastating volume change, the structured AEMHs can easily break into powders, resulting in uncontrollable performance and potential safety risk to the vehicles [10,15]. Furthermore, the endothermic reaction of ammonia release from the metal amine complex requires buffering time for the heating, leading to NO_x emission in the first 5-10 min in the cold start of the automotive engines [16]. Therefore,

Selection and peer-review under responsibility of the scientific committee of the 13th Int. Conf. on Applied Energy (ICAE2021).

a structure-reliable ammonia carrier with rapid sorption kinetics is one of the keys to promote ammonia-based environmental and energy applications.

Zeolites containing micropores are popular gas sorbents with excellent structural stability and rapid kinetics in gas sorption [17]. Zeolite NaX (faujasite), as one of the massively produced zeolites, possesses a high surface area, indicating promising ammonia capacity [18]. In this work, we have designed a three-dimensional (3D) printed zeolite NaX-$MgCl_2$ unit as potential ammonia carriers by a pressure-assisted microsyringe approach. The designed unit contains a NaX scaffold and $MgCl_2$ blocks, where the NaX provides the cages for $MgCl_2$ "breathing" during ammonia sorption cycles, as illustrated in Fig. 1. Our design and results offer a solution to combine the chemisorption and physisorption of ammonia and open a new view to structure the zeolite-AEMHs composites by 3D printing method for ammonia storage applications.

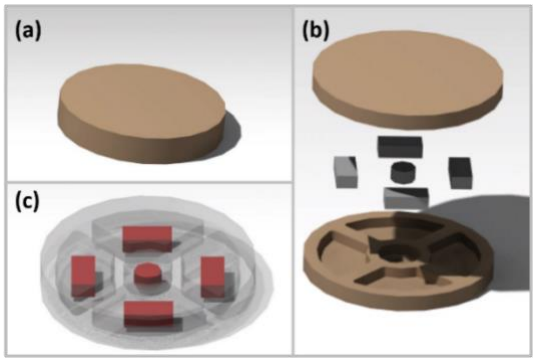

Fig. 1 Schematic illustration of the 3D-printed NaX-$MgCl_2$ unit, consisting of the zeolite NaX scaffold and the $MgCl_2$ blocks inside the cages of the scaffold.

2. EXPERIMENTAL

2.1 Materials and ink preparation

Zeolite NaX powder (2-4 µm, Luoyang Jianlong Chemical Industry Co., Ltd), magnesium chloride (anhydrous, 99 % purity, Alfa Aesar), bentonite clay (Sigma-Aldrich), polyvidone (PVP) (Alfa Aesar) were mixed with a speed mixer (Synergy Devices Ltd., UK) at 3000 rpm for 4 min with different formulations as shown in Table 1.

2.2 Rheology characterization

The rheological properties of the prepared ink were characterized with a rheometer (Discovery H2, TA instruments, USA). The amplitude sweeps were performed from 0.0001 Pa.s shear rate to 10000 Pa.s using 10 rad s^{-1} oscillation speed to determine the viscoelastic regime of the inks. After that, the viscosity of the ink was measured with 0.001 Pa.s to 1000 Pa.s shear rate for 1 min with 10 points per logarithmic scale.

2.3 3D printing samples preparation

The 3D printing method in this work is pressure-assisted microsyringe (PAM) by a Bio-printer (Inkredible+, Cellink, USA), which includes two print heads actuated with compressed air. The nozzles for the zeolite scaffold and $MgCl_2$ were 800 microns and 1.2 mm, respectively. The geometry of the sample was designed in CARIA V5 software and then converted into G-code with the Slic3r software for printing.

The printed zeolite scaffold was heated up to 700 °C in the box furnace (Nabertherm, Germany) at 5 °C min^{-1} to remove the organic binders.

2.4 Structural characterization

The microstructure of the 3D-printed zeolite scaffold was characterized by scanning electron microscopy (SEM, JSM-IT300LV, JEOL GmbH, Germany). The phase of the NaX scaffold before and after heat treatment was characterized by a Cu Kα radiation X-ray diffractometer (Empyrean, PANalytical, UK). The Brunauer–Emmett–Teller (BET) surface area of the samples was measured by N_2 adsorption at liquid nitrogen temperature (-196 °C) by a surface area analyzer (Gemini VII 2390, Micromeritics, USA), with sample-degassing pretreatment at 300 °C, high vacuum overnight.

2.5 Ammonia adsorption-desorption measurement

The ammonia adsorption-desorption performance was characterized by a simultaneous thermal analyzer (SDT650, TA instruments, USA). The obtained NaX scaffold and $MgCl_2$ blocks were first degassed at 300 °C, and once the specimens cooled down to 25 °C, the protective argon gas was cut off following with a 100 mL min^{-1} NH_3 flow for the adsorption measurement until saturation. Ammonia desorption was measured at 35 °C to simulate the low-temperature scenarios of the cold start of the vehicles.

Table 1 List of the formulations of different inks

Sample Code	NaX	PVP	H2O	Bentonite
InkBase	0	20	80	0
Ink1	10	18	72	0
Ink2	20	16	64	0
Ink3	30	14	56	0
Ink4	40	12	48	0
Ink5	50	10	40	0
Ink-Final	50	10	35	5

3. RESULTS AND DISCUSSION

3.1 Ink selection with rheological characterization

To optimize and select the ink suitable for printing NaX scaffold, a series of rheological measurements were performed on different formulations as listed in Table 1. The relationship between the shear rate and viscosity was studied, as shown in Fig. 2(a). Compared with other tested inks, Ink5 presented shear thinning behavior, where it has high viscosity at a low shear rate and low viscosity at a high shear rate [19]. In such a case, the ink can easily extrude through the nozzle tips by applying shear stress and maintain the designed morphology with its high viscosity at a low shear rate [20].

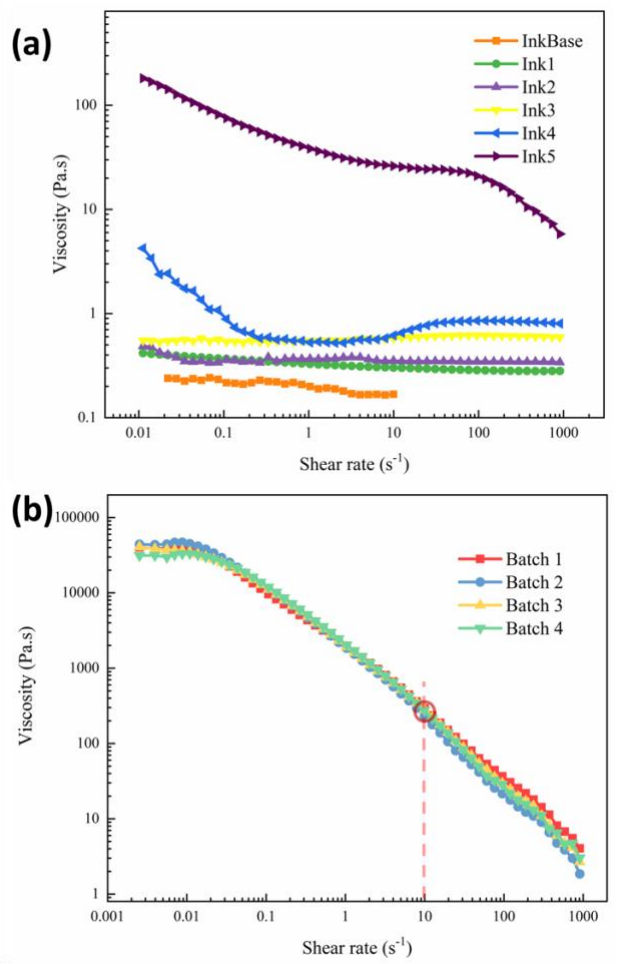

Fig. 2 (a) The shear rate vs. viscosity curves of the formulated inks (Table 1); (b) The shear rate vs. viscosity curves for Ink-Final in 4 different batches.

Considering the rheological performance, the high NaX loading target, and binder for the mechanical performance, we formulated Ink-Final for the NaX scaffold printing. The Ink-Final presented a reliable and repeatable rheological performance with different batches, as shown in Fig. 2(b). Following the rheological behavior, a shear rate of 10 s^{-1} marked by a circle in Fig. 2(b) was used for the 3D printing, as the viscosity of the Ink-Final remains above 100 Pa.s, bringing mechanical stability to the printed structure for drying.

3.2 Structural characterization

The printed NaX scaffold demonstrated excellent structural stability and maintained the geometry after thermal treatment, as shown in the specimen photos in Fig. 3. The organic binders were removed by the thermal treatment, where the white scaffold turned into black color by the carbonization of the polymer after 500 °C, where the carbon flakes can be observed in the SEM images in Fig. 3(b)-(c). The carbon was eliminated when heating up to 700 °C, where the scaffold turned back to light color. The bentonite linked the zeolite particles, as shown in the SEM image in Fig. 3(d), offering stable mechanical performance while handling and do not show defects like micro and macroscopic cracks. The XRD pattern in Fig. 3(e) confirmed the 3D-printed NaX scaffold before and after 700 °C thermal treatment possesses characteristic peaks as the raw NaX powder, suggesting no damage in the crystal structure by the fabrication process.

3.3 Ammonia sorption characterization

The measured ammonia uptake capacity of raw $MgCl_2$ and the obtained NaX scaffold was 58.7 mmol g^{-1} and 8.8 mmol g^{-1}, respectively. In the ammonia sorption percentage curves, the NaX scaffold could offer faster kinetics in ammonia absorption, where it took 1 min to reach 90% saturated uptake, 10 times faster than 11 min in the $MgCl_2$, as shown in Fig. 4(a). Furthermore, during the ammonia desorption at low temperature (35 °C), the NaX scaffold released 40% ammonia uptake (approximately 3.5 mmol g^{-1}) in the first 10 min, which was 50% higher than the $MgCl_2$ of 4% (approximately 2.3 mmol g^{-1}). The rapid kinetics in the NaX scaffold in the low-temperature regime is due to the physisorption mechanism, where NaX scaffold possesses BET surface area of 335 m^2 g^{-1}, much higher than 3 m^2 g^{-1} of the $MgCl_2$ [13,21].

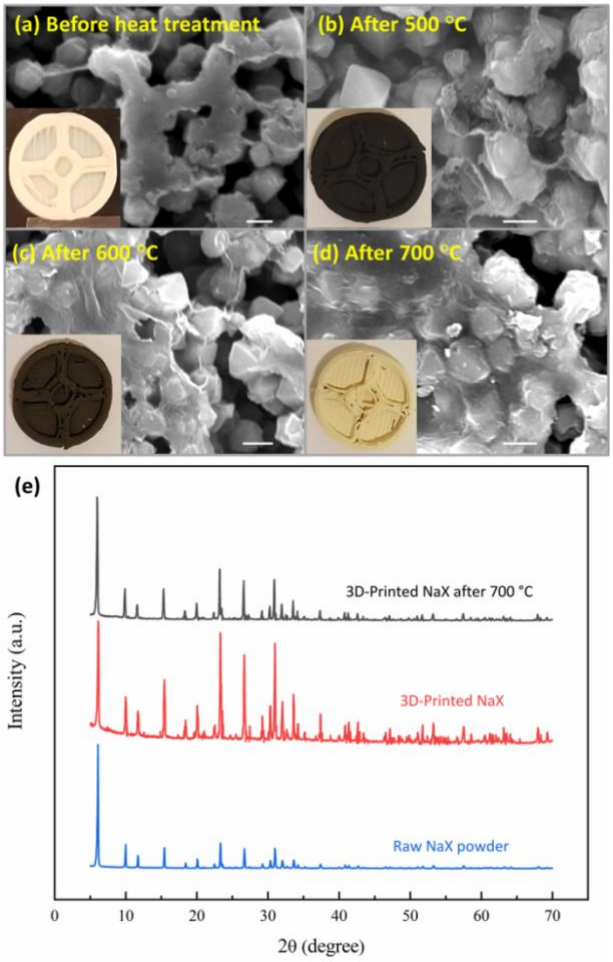

Fig. 3 SEM images of 3D-printed NaX scaffold, scale bar, 2 µm, (a) before heat treatment; (b) after 500 °C; (c) after 600 °C; (d) after 700 °C; (e) XRD pattern of the raw NaX powder and the printed specimen before and after 700 °C thermal treatment.

In the designed unit, the NaX scaffold can start to offer the ammonia dosing at low temperature to minimize the buffering time, and once the cartridge reaches the decomposition temperature of $Mg(NH_3)_6Cl_2$ at 135 °C, the $MgCl_2$ can contribute the most ammonia dosing with its superior ammonia capacity.

The follow-up plan is to co-print the $MgCl_2$ blocks by the second micro-syringe, where the optimized $MgCl_2$ ink formula still requires further study. One alternative approach is to use compression blocks, as reported in other studies [13,22]. It is interesting to measure the ammonia sorption performance as a unit with a suitable set up in future study.

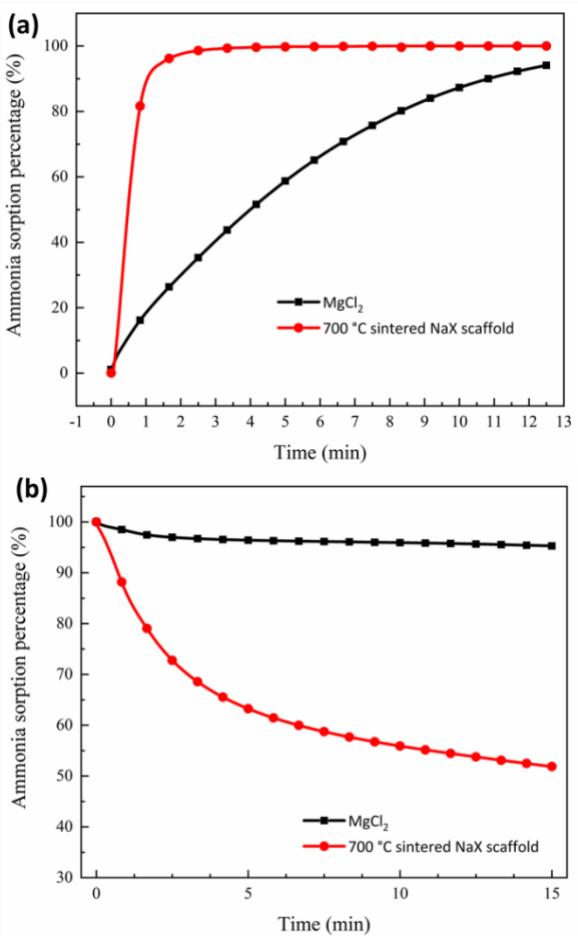

Fig. 4 The ammonia sorption percentage of the $MgCl_2$ particles and 700 °C sintered NaX scaffold, (a) adsorption; (b) desorption.

4. CONCLUSION

A 3D-printed NaX unit was designed to carry $MgCl_2$ as enhanced ammonia carriers for SCR systems. The 3D-printing ink for the NaX scaffold was optimized with the rheological study. The printed NaX scaffold demonstrated stable mechanical strength and superior ammonia sorption kinetics at low-temperature regime. Combining the physisorption and chemisorption from NaX and $MgCl_2$, respectively, can reduce the NO_x emission and bring a net-zero expansion structure to the ammonia storage and delivery system. Our approach opens a view for applying the 3D-printing method to combine various materials for ammonia storage and promote the potential ammonia as clean fuel applications.

ACKNOWLEDGEMENT

This work was funded by Formas with project number 2016-01099. The authors acknowledge Dr. Mohammed Elbadawi for his help and consult of the rheology and 3D-printing experiments.

REFERENCE

[1] Copat C, Cristaldi A, Fiore M, Grasso A, Zuccarello P, Signorelli SS, et al. The role of air pollution (PM and NO2) in COVID-19 spread and lethality: A systematic review. Environmental Research 2020;191:110129. https://doi.org/10.1016/j.envres.2020.110129.

[2] Ogen Y. Assessing nitrogen dioxide (NO2) levels as a contributing factor to coronavirus (COVID-19) fatality. Science of The Total Environment 2020;726:138605. https://doi.org/10.1016/j.scitotenv.2020.138605.

[3] Cao Z, Akhtar F. Porous Strontium Chloride Scaffolded by Graphene Networks as Ammonia Carriers. Advanced Functional Materials n.d.;n/a:2008505. https://doi.org/10.1002/adfm.202008505.

[4] Klerke A, Christensen CH, Nørskov JK, Vegge T. Ammonia for hydrogen storage: challenges and opportunities. Journal of Materials Chemistry 2008;18:2304. https://doi.org/10.1039/b720020j.

[5] Hviid Christensen C, Zink Sørensen R, Johannessen T, J. Quaade U, Honkala K, D. Elmøe T, et al. Metal ammine complexes for hydrogen storage. Journal of Materials Chemistry 2005;15:4106–8. https://doi.org/10.1039/B511589B.

[6] Godfrey HGW, da Silva I, Briggs L, Carter JH, Morris CG, Savage M, et al. Ammonia Storage by Reversible Host–Guest Site Exchange in a Robust Metal–Organic Framework. Angewandte Chemie International Edition 2018;57:14778–81. https://doi.org/10.1002/anie.201808316.

[7] Yim SD, Kim SJ, Baik JH, Nam I, Mok YS, Lee J-H, et al. Decomposition of Urea into NH3 for the SCR Process. Ind Eng Chem Res 2004;43:4856–63. https://doi.org/10.1021/ie034052j.

[8] Szymaszek A, Samojeden B, Motak M. The Deactivation of Industrial SCR Catalysts—A Short Review. Energies 2020;13:3870. https://doi.org/10.3390/en13153870.

[9] Damma D, Ettireddy PR, Reddy BM, Smirniotis PG. A Review of Low Temperature NH3-SCR for Removal of NOx. Catalysts 2019;9:349. https://doi.org/10.3390/catal9040349.

[10] Elmøe TD, Sørensen RZ, Quaade U, Christensen CH, Nørskov JK, Johannessen T. A high-density ammonia storage/delivery system based on Mg(NH3)6Cl2 for SCR–DeNOx in vehicles. Chemical Engineering Science 2006;61:2618–25. https://doi.org/10.1016/j.ces.2005.11.038.

[11] Liu CY, Aika K. Ammonia Absorption into Alkaline Earth Metal Halide Mixtures as an Ammonia Storage Material. Industrial & Engineering Chemistry Research 2004;43:7484–91. https://doi.org/10.1021/ie049874a.

[12] Sharonov VE, Aristov YI. Ammonia adsorption by MgCl2, CaCl2 and BaCl2 confined to porous alumina: the fixed bed adsorber. React Kinet Catal Lett 2005;85:183–8. https://doi.org/10.1007/s11144-005-0259-5.

[13] Cao Z, Grimaldos Osorio N, Cai X, Feng P, Akhtar F. Carbon-reinforced MgCl2 composites with high structural stability as robust ammonia carriers for selective catalytic reduction system. Journal of Environmental Chemical Engineering 2020;8:103584. https://doi.org/10.1016/j.jece.2019.103584.

[14] Jacobsen HS, Hansen HA, Andreasen JW, Shi Q, Andreasen A, Feidenhans'l R, et al. Nanoscale structural characterization of Mg(NH3)6Cl2 during NH3 desorption: An in situ small angle X-ray scattering study. Chemical Physics Letters 2007;441:255–60. https://doi.org/10.1016/j.cplett.2007.05.001.

[15] Yuan Z, Khakzad N, Khan F, Amyotte P. Dust explosions: A threat to the process industries. Process Safety and Environmental Protection 2015;98:57–71. https://doi.org/10.1016/j.psep.2015.06.008.

[16] Myung C-L, Jang W, Kwon S, Ko J, Jin D, Park S. Evaluation of the real-time de-NO x performance characteristics of a LNT-equipped Euro-6 diesel passenger car with various vehicle emissions certification cycles. Energy 2017;132:356–69. https://doi.org/10.1016/j.energy.2017.05.089.

[17] Cheung O, Bacsik Z, Liu Q, Mace A, Hedin N. Adsorption kinetics for CO2 on highly selective zeolites NaKA and nano-NaKA. Applied Energy 2013;112:1326–36. https://doi.org/10.1016/j.apenergy.2013.01.017.

[18] Matito-Martos I, Martin-Calvo A, Ania CO, Parra JB, Vicent-Luna JM, Calero S. Role of hydrogen bonding in the capture and storage of ammonia in zeolites. Chemical Engineering Journal 2020;387:124062. https://doi.org/10.1016/j.cej.2020.124062.

[19] Thakkar H, Lawson S, Rownaghi AA, Rezaei F. Development of 3D-printed polymer-zeolite composite monoliths for gas separation. Chemical Engineering Journal 2018;348:109–16. https://doi.org/10.1016/j.cej.2018.04.178.

[20] Lefevere J, Protasova L, Mullens S, Meynen V. 3D-printing of hierarchical porous ZSM-5: The importance of the binder system. Materials & Design 2017;134:331–41. https://doi.org/10.1016/j.matdes.2017.08.044.

[21] Cao Z, Landström KN, Akhtar F. Rapid Ammonia Carriers for SCR Systems Using MOFs [M2(adc)2(dabco)] (M = Co, Ni, Cu, Zn). Catalysts 2020;10:1444. https://doi.org/10.3390/catal10121444.

[22] Zhu H, Gu X, Yao K, Gao L, Chen J. Large-Scale Synthesis of MgCl2·6NH3 as an Ammonia Storage Material. Ind Eng Chem Res 2009;48:5317–20. https://doi.org/10.1021/ie900177q.